Design of Chemoresistive Sensory Materials: Polythiophene-Based Pseudopolyrotaxanes

Michael J. Marsella, Patrick J. Carroll, and Timothy M. Swager*

Contribution from the Department of Chemistry and Laboratory for Research on the Structure of Matter, University of Pennsylvania, Philadelphia, Pennsylvania 19104-6323

Received May 24, 1995[⊗]

Abstract: Herein we report conducting polymer-based sensors which transduce reversible, noncovalent, and non-redox-dependent molecular recognition events into measurable changes in conductivity. These chemoresistive polymers are derived from bithiophenes containing cyclophane receptors capable of forming self-assembled pseudorotaxane complexes with paraquat. The electrostatic perturbations arising from pseudopolyrotaxane formation cause a decrease in carrier mobility and thus lower the conductivity. The chemoresistive response was found to be consistent with decreased carrier mobility and exhibited an enhanced sensitivity to analyte-promoted electrostatic perturbations relative to the voltammetric response. Polymer-based devices which demonstrate a real time chemoresistive response to paraquat are also reported.

Introduction

A practical molecule-based sensory device must efficiently transduce molecular interactions into a readily measurable response. Such a device requires molecular recognition events occurring at receptors which have been designed such that different properties emanate from occupied and unoccupied states.[1] Established examples of molecular sensory components are crown ether dyes which exhibit changes in absorbance upon binding ions.[1] Increased sensitivity in such a system requires an increase in the binding energy between receptor and guest. However, a sufficiently large association constant (K_a) leads to a compromised reversibility which precludes the formation of sensory devices which function in real time with varying analyte concentrations. To avoid this problem, we are pursuing an alternate route to enhanced sensitivity in which the magnitude of response emanating from analyte occupied receptors is amplified. Our approach is conceptualized in Scheme 1, wherein multiple molecular recognition sites are "wired in series" such that analyte binding at just one site can affect a specific measurable property of the entire molecular wire. The key to realizing amplification in the connected receptor system (Scheme 1b) relative to the isolated receptor molecules (Scheme 1a) is to choose a measurable property which depends not on a single unit but the collective system. One such property is electrical conduction. Hence an increased resistance in only one segment of a molecular wire will raise the resistance of the entire system.

In our systems, electrically conducting polymer (CP) chains serve as the molecular wires to which receptors are covalently attached. It is known that the conductivity of CPs can vary by several orders of magnitude in response to even minor perturbations in the chemical structure, oxidation state, electronic environment, and/or solid state ordering of the material.[2] As such, we postulated that the conductivity of CPs should be dramatically affected by perturbations resulting from even low populations of occupied receptor sites. Additionally, monitoring changes in conductivity requires minimal electronics and is thus an attractive and practical sensory response mechanism. In this paper, we demonstrate the utilization of molecular recognition to harness the large dynamic range of conductivity in CPs and translate it into a useful sensory probe.

While substrate-selective chemoresistive materials based on enzyme-CP composites have been previously reported, these materials function on chemically irreversible redox events.[3,4] Such an irreversible sensing mechanism produces a time-dependent (nonequilibrium) response, and as such, these materials must be "reset" back to their original state either chemically or by potentiostatic control. As a result, more sophisticated electronic/measurement protocols are required to obtain a real-time response. We chose to avoid the use of such sophisticated electronics by designing chemoresistive sensory materials that do not function on redox-mediated changes in conductivity. Access to such a system can be easily understood from the description of conductivity (σ):

$$\sigma = ne\mu$$

where n is the number of carriers (a function of oxidation state), e is the carrier's charge, and μ is carrier mobility. Our focus here is on attenuating σ by controlling μ. This can be achieved by erecting barriers to carrier transport via electrostatic repulsions between the bipolaronic carriers and receptor-bound analytes. A key feature of our approach is that n remains constant; thus no redox chemistry is required to alter conductivity.

Perhaps of even greater significance is the potentially higher sensitivity of chemoresistivity as compared with other observable responses such as changes in cyclic voltammetry and/or the UV-visible spectrum. This effect originates from the cooperative nature of carrier transport in a CP (Scheme 1), in which microscopic perturbations anywhere along the carrier's path can impede its bulk mobility. In contrast, it is known that both the potential at which a CP is oxidized and its optical properties are controlled by the localized electronic structure of the polymer.[2] For example, cyclic voltammograms and UV-visible spectra of low molecular weight oligothiophenes are very similar to those of high molecular weight polythiophenes.[2] In

[⊗] Abstract published in *Advance ACS Abstracts*, September 1, 1995.

(1) *Supramolecular Chemistry I—Directed Synthesis and Molecular Recognition*; Weber, E., Ed.; Springer-Verlag: New York, 1993.

(2) *Handbook of Conducting Polymers*; Skotheim, T. J., Ed.; Dekker: New York, 1986.

(3) Bartlett, P. N.; Birkin, P. R. *Synth. Met.* **1993**, *61*, 15.

(4) For a recent review, see: Swager, T. M.; Marsella. M. J. *Adv. Mater.* **1994**, *6*, 595.

0002-7863/95/1517-9832$09.00/0

Scheme 1

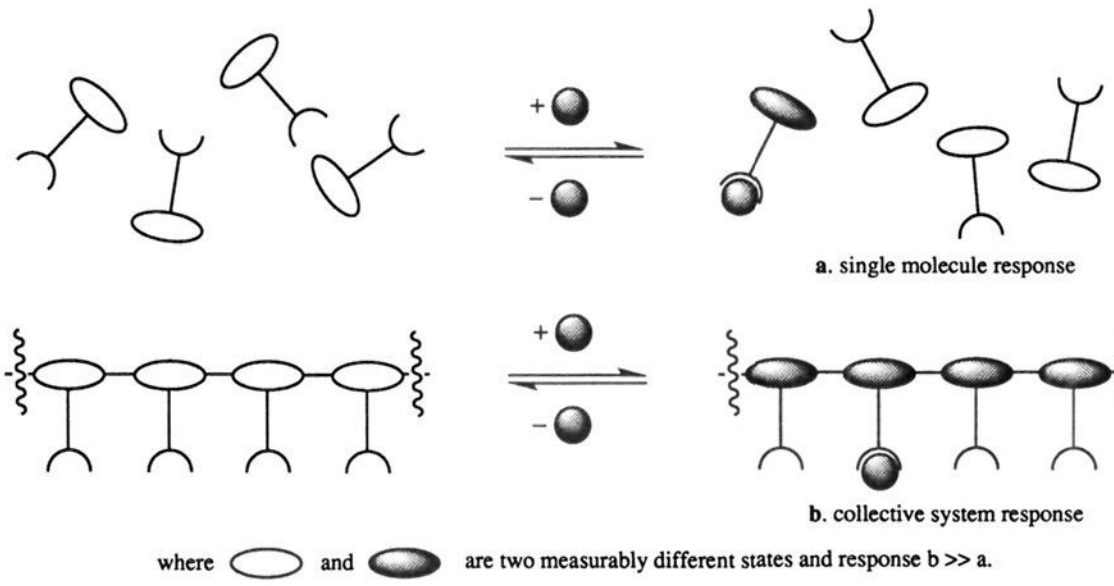

Scheme 2

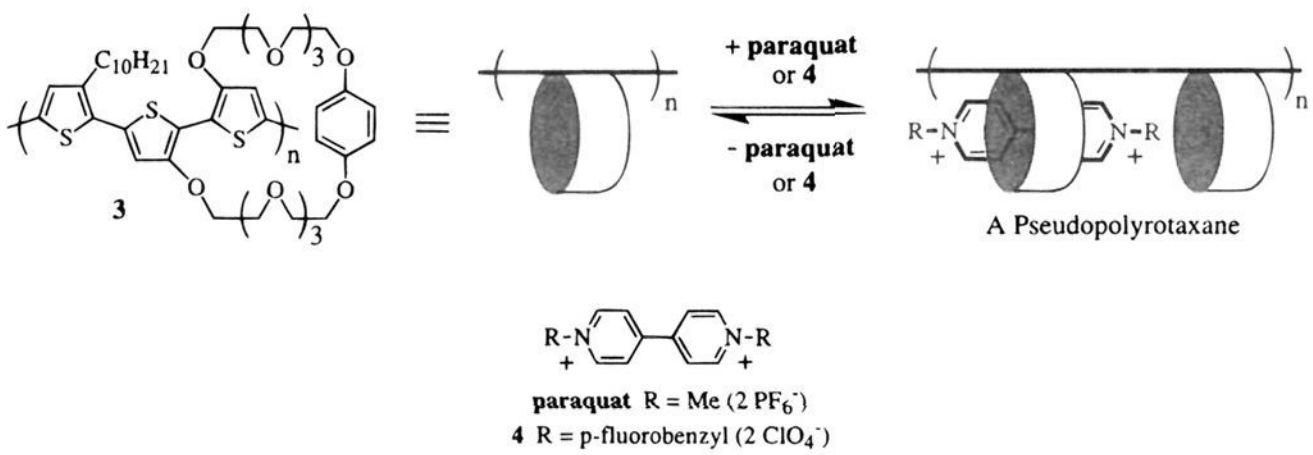

contrast, bulk conductivity is highly dependent on long-range carrier mobility; thus, even minor perturbations occurring in the CP which impede carrier mobility will produce a reduction in conductivity. As such, conductivity can be utilized as a probe which effectively amplifies the detection of perturbations occurring at local sites along the polymer chain.

To conceptually illustrate this amplification effect, consider a conducting polymer in which each repeat unit possesses a receptor site (Scheme 1b). In its conducting state, the carrier species migrates along the polymer chain, essentially "sampling" each receptor. In the ideal case of isolated chains (i.e., no interchain hopping), occupation of a single receptor site by a guest which inhibits the carrier's mobility will be reflected by a decrease in conductivity. The sensitivity of transport phenomena to local perturbations is potentially very general, and we have recently reported conjugated polymer-based fluorescent chemosensors based upon energy transport which display a greatly enhanced sensory response with respect to monomeric analogs.[5]

Substituted polythiophenes are an ideal choice from which to produce chemoresistive sensory materials as a result of their high conductivity, environmental stability, and relative ease of structural modification.[6,7] In our previous works, we have demonstrated that covalent attachment of receptor sites across the 3,3′ positions of a bithiophene repeat unit is an excellent way to translate molecular recognition events into conformational and/or electrostatic perturbations within the polymer.[8,9] Systems developed on the basis of this (and similar) methodology have demonstrated reversible ionochromic, voltammetric, fluorescent, and both iono- and chemoresistive responses.[8-10]

Our earlier investigations into a paraquat-selective chemoresistor focused on **1**, a macrocyclic bithiophene monomer designed to mimic bis(*p*-phenylene)-34-crown-10's (**2**) ability to form self-assembled charge-transfer complexes with paraquat.[9] As shown, the structural similarities between **1** and **2** when the bithiophene unit of **1** is in a transoid configuration are readily apparent.

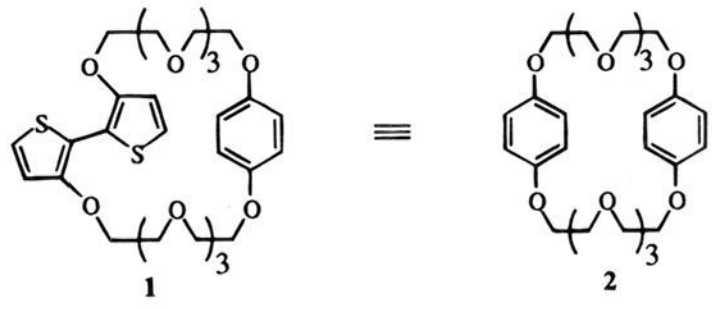

Although complexation-induced shifts in the redox potential of monomeric pseudorotaxane complexes have been previously reported,[11] our earlier investigations of the pseudopolyrotaxane complex of polymer **3** with paraquat showed no change in the polymer's redox potential (Scheme 2). Initially underestimating the amplification effect, we incorrectly made the assumption that a chemoresistive response requires a commensurate voltammetric response. Therefore, we did not investigate the chemoresistive properties of **3** as a function of paraquat. However, we demonstrated both the desired voltammetric and chemoresistive responses with exposure of **3** to the more electron deficient paraquat analog, **4**.

In a related effort involving ionoresistive polythiophenes reported in the paper immediately following this one, we have discovered that there appears to be no direct correlations between

(5) Zhou, Q.; Swager, T. M. *J. Am. Chem. Soc.* **1995**, *117*, 7017.
(6) Roncali, J. *Chem. Rev.* **1992**, *92*, 711.
(7) Heywang, G.; Jonas, F. *Adv. Mater.* **1992**, *4*, 116.
(8) Marsella, M. J.; Swager, T. M. *J. Am. Chem. Soc.* **1993**, *115*, 12214.
(9) Marsella, M. J.; Carroll, P. J.; Swager, T. M. *J. Am. Chem. Soc.* **1994**, *116*, 9347.
(10) See: Marsella, M. J.; Newland, R. J.; Carroll, P. J.; Swager, T. M. *J. Am. Chem. Soc.* **1995**, *117*, 9842 (following paper in this issue).
(11) Bernardo, A. R.; Stoddart, J. F.; Kaifer, A. E. *J. Am. Chem. Soc.* **1992**, *114*, 10624.

Scheme 3[a]

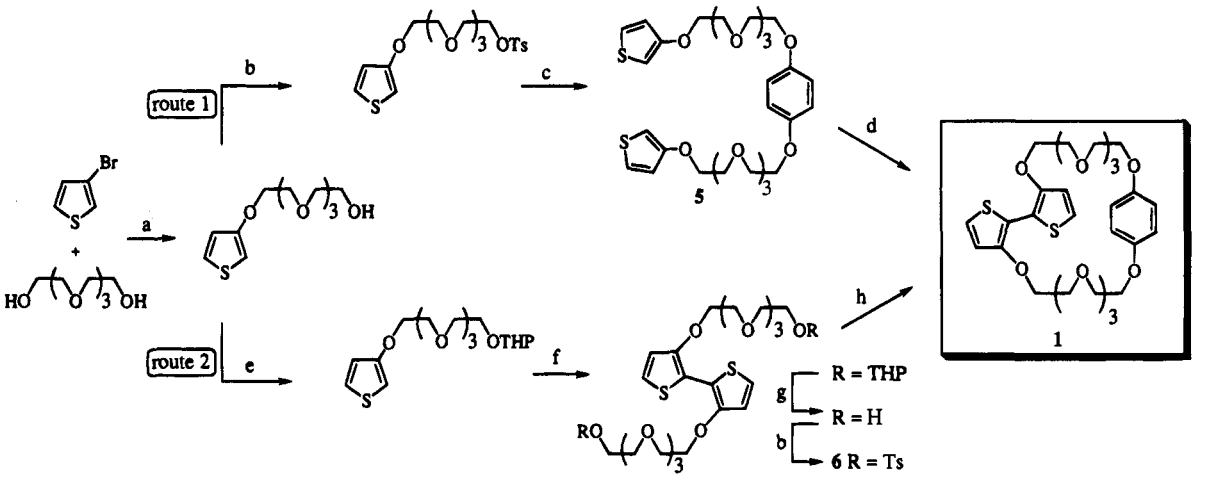

[a] (a) *t*-BuOK, 0.2 equiv of CuI, pyridine, reflux (69%); (b) *p*-TosCl, pyridine, 0 °C (95% route 1; 77% route 2); (c) 0.5 equiv of hydroquinone, K_2CO_3, acetone, DMF, reflux (95%); (d) (1) 2 equiv of BuLi, THF, 0 °C; (2) 2 equiv of Fe(acac)$_3$, THF, reflux (13%); (e) dihydropyran, pyrH$^+$Tos$^-$, CH_2Cl_2 (90%); (f) (1) BuLi, THF, 0 °C; (2) Fe(acac)$_3$, THF, reflux (69%); (g) pyrH$^+$Tos$^-$, MeOH (100%); (h) 1 equiv of hydroquinone, Ce_2CO_3, DMF, 50 °C (17%).

Scheme 4[a]

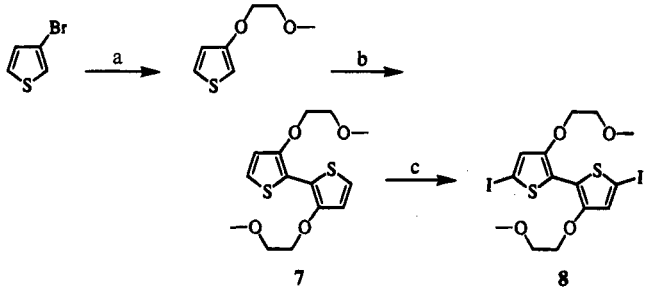

[a] (a) HO(CH$_2$)$_2$OMe, *t*-BuOK, 0.2 equiv of CuI, lutidine, 100 °C (78.4%); (b) (1) 1 equiv of BuLi, THF, 0 °C; (2) Fe(acac)$_3$, THF, reflux (70%); (c) (1) 2 equiv of Hg(OAc)$_2$, CH_2Cl_2, no *hν*; (2) 2 equiv of NIS, CH_2Cl_2, no *hν* (60%).

the chemoresistive response and changes in the potential at which a polymer is oxidized. These results have provided insight into the amplification process and prompted us to re-examine the paraquat-induced chemoresistive properties of **3** and related polymers, the results of which are reported herein.

Results and Discussion

a. Synthesis and Characterization of Monomers and Polymers. Macrocycle **1** was synthesized from commercially available 3-bromothiophene by two independent routes (Scheme 3). The key difference between the two strategies lies in the final macrocyclization step. Route 1 makes use of the ability of the oxygen directly attached to the 3-position of the thiophene to direct lithiation by *n*-butyllithium to the 2-position of **5**. The macrocycle is then established by Fe(acac)$_3$ oxidative coupling of the dilithio species of **5**. In route 2, the bithiophene unit is formed prior to macrocyclization of **6** via a cesium ion-templated Williamson ether synthesis. The overall yield for macrocycle **1** via route 1 is 8.1%, which is a slightly higher yield than that obtained by route 2.

The ability of **1** to form strong self-assembled complexes with paraquat is immediately apparent from the resulting dark red solution which is observed upon mixing the two white solids in acetone or acetonitrile. It is important to note that the resultant charge-transfer complex is only observed for the macrocyclic complexes and is not present under similar conditions with the model compound, **7** (Scheme 4). Standard UV–vis spectroscopic techniques were utilized to determine the strength of paraquat binding of **1** relative to that of **2**. The K_a for **1** was determined to be 1360 M^{-1}, approximately twice the K_a reported for **2** (730 M^{-1}).[12] This difference may be accounted for by the more electron rich nature of the dialkoxybithiophene moiety which results in stronger charge-transfer interactions with paraquat.

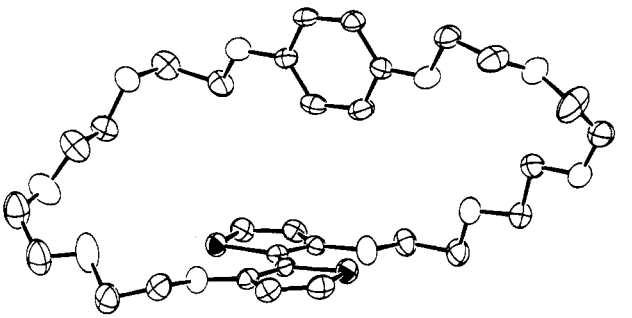

Figure 1. ORTEP representation of **1** with 30% probability thermal ellipsoids displayed.

In an effort to better understand the conformational perturbations introduced onto the bithiophene upon "rotaxification", crystals of **1** and the corresponding pseudorotaxane complex were structurally characterized. We have previously reported the ORTEP drawing of the pseudorotaxane complex of **1** with paraquat which shows the bithiophenes lying in a planar transoid conformation.[9] The ORTEP drawing of **1** in its unoccupied state is shown in Figure 1 and demonstrates that the transoid configuration and relative planarity of the bithiophene unit (4.4° dihedral angle between thiophenes) are maintained in both states. This indicates that any observed chemoresistive response is primarily due to electrostatic and not conformational perturbations.

The macrocycle containing polymers **3** and **9** and the non-macrocyclic model polymer **10** were synthesized as shown in Scheme 5. Although the macrocyclic 3,3′-dialkoxybithiophene monomer is the design of choice, these systems have been problematic in both synthetic and electrochemical polymerization protocols. As is generally the case in 3-alkoxythiophenes, **1** is not effectively polymerized by electrochemical oxidation.[6]

(12) Allwood, B. L.; Spencer, N.; Shahriari-Zavareh, H.; Stoddart, J. F.; Williams, D. J. *J. Chem. Soc., Chem. Commun.* **1987**, 1064.

Scheme 5[a]

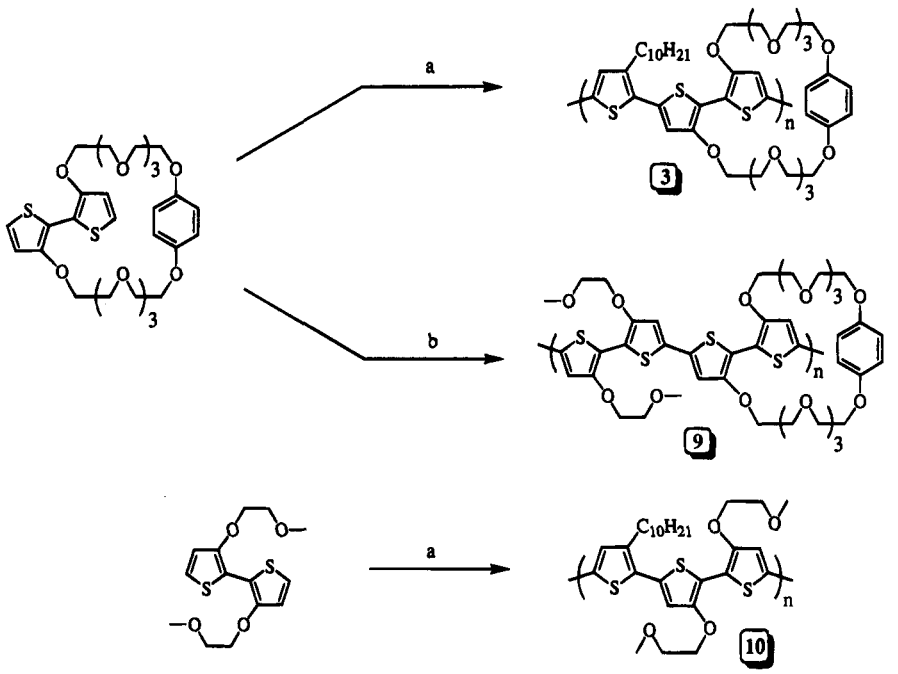

[a] (a) (1) 2 equiv of BuLi, 10 equiv of LiCl, THF, 0 °C, sonicate; (2) 2.2 equiv of $ZnCl_2$, THF; (3) 1 equiv of 3-decyl-2,5-dibromothiophene, 3% $Pd(PPh_3)_4$; (b) (1) 2.1 equiv of BuLi, 10 equiv of LiCl, THF, 0 °C, sonicate; (2) 2.2 equiv of Me_3SnCl, THF; (3) 1 equiv of **8**, 3% $Pd(PPh_3)_4$, DMF.

In addition, due to its high reactivity, we were unable to isolate halide or stannane derivatives as pure compounds for use in subsequent cross-coupling polymerization schemes. These synthetic restrictions limited us to *in situ* generation of monomers for cross-coupling polymerizations in which complete dilithiation of **1** was critical for obtaining polymers with reasonable molecular weights. This was accomplished by lithiation with stoichiometric *n*-butyllithium in the presence of excess LiCl and accompanied by sonication. Subsequent transmetalation with $ZnCl_2$ followed by a palladium-catalyzed copolymerization with 2,5-dibromo-3-decylthiophene produced polymer **3** in >98% yield (M_n = 6500).

In an attempt to increase polymer−paraquat interactions, we designed a second polymer (**9**) to posses the ability to be oxidized at a potential lower than that of **3**. We reasoned that the chemoresistive response would be greater for a polymer which is oxidized at a potential close to that at which paraquat is reduced, since such a situation produces increased charge-transfer interactions. To achieve this goal, the 3-decylthiophene moiety of **3** was replaced with 3,3′-bis(methoxyethoxy)-2,2′-bithiophene (**7**). This monomer, which was originally synthesized as a non-macrocyclic analog of **1**, was chosen on the basis of the fact that alkoxy-substituted polythiophenes are oxidized at potentials lower than those of their corresponding alkyl derivatives.

For the synthesis of **9**, we attempted to improve on our earlier *in situ* protocol. Thus, lithiation of **1** was carried out as before, with the exception that a slight excess of *n*-butyllithium was used to ensure complete dilithiation. The organolithium compounds were then quenched with trimethyltin chloride to produce the bis(trimethylstannyl) derivative of **1** and convert the residual *n*-butyllithium to the relatively inert *n*-butyltrimethyltin. The polymerization then proceeded via a palladium-catalyzed Stille-type cross-coupling of the organotin derivative with **8**.[13] Although this protocol only produced polymers with modest molecular weight (M_n = 3800), quality thin films of this polymer could be cast from chloroform. It should be noted that high molecular weight is not a prerequisite for high conductivity in polythiophenes. In fact, low molecular weight thiophene oligomers can display greater crystallinity and, as a result, may exhibit higher conductivities than larger, disordered polymers.[14] This may be especially true in alkoxy-substituted thiophenes which typically demonstrate rigid planarity and increased packing stability.[15] In fact, Leclerc and co-workers have demonstrated poly(3,3′-dibutoxy-2,2′-bithiophene), with a degree of polymerization of ca. 10, to exhibit a conductivity of 2 S/cm upon chemical doping with $FeCl_3$.[16]

For comparative purposes, a model polymer (**10**) which lacked a molecular recognition site was also synthesized (M_n = 12 000). Although this polymer more closely resembles **3** in structure, its redox properties are closer to those observed in polymer **9**. The difference is particularly apparent by comparing the potential at which the peak anodic current ($E_{p,a}$) of the polymers is observed. For both **9** and **10**, $E_{p,a}$ corresponds to relatively low potentials (ca. −0.12 V vs Ag wire) with respect to **3** (ca. +0.15 V vs. Ag wire). These results are most likely a reflection of the advantageous incorporation of **7** in both **9** and **10**.

Realizing that **7** contributed significantly to the reduced redox potentials exhibited by **9** and **10**, we theorized that in addition to its electron-donating nature it must also lie rigidly planar. To understand the conformational preference of this moiety, crystals of **7** were isolated and structurally characterized. The ORTEP drawing is shown in Figure 2. The transoid planar structure further supports work by others who have shown that alkoxy side chains on polythiophenes do not disturb the planarity of the main chain.[15] In this regard, we propose that the regiorandom (H−H and H−T) orientations of the decyl chains in polymer **3** interact unfavorably with their neighboring environments, thus introducing significant twisting of the polymer backbone and increasing the potential at which it is

(13) Stille, J. K. *Angew. Chem., Int. Ed. Engl.* **1986**, *25*, 508.

(14) Hartel, M.; Kossmehl, G.; Manecke, W.; Willie, D.; Wöhrle, D.; Zerpner, D. *Angew. Makromol. Chem.* **1973**, *29/30*, 307.

(15) Meille, S.; Farina, A.; Bezziccheri, F.; Gallazzi, M. *Adv. Mater.* **1994**, *6*, 848.

(16) Faïd, K.; Cloutier, R.; Leclerc, M. *Macromolecules* **1993**, *26*, 2501.

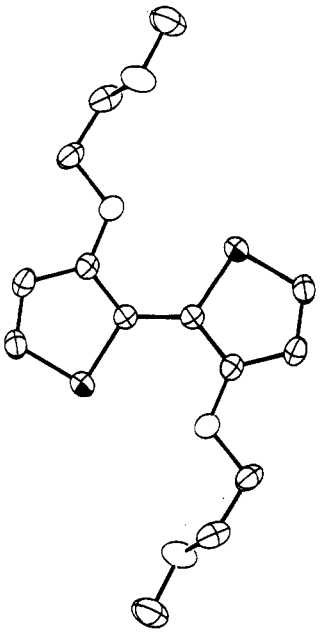

Figure 2. ORTEP representation of **7** with 30% probability thermal ellipsoids displayed.

oxidized. In contrast, the comparatively lower potential at which polymers **9** and **10** are oxidized results from both the increased planarity and the increased electron-donating ability of **7**.

b. Electrochemical Measurements. Electrochemical studies were performed using devices fabricated by solution casting the polymer of interest onto an array of two platinum interdigitated microelectrodes having an interelectrode spacing of 10 μm. Cyclic voltammetry was performed by maintaining both electrodes at the same potential. Relative conductivity measurements were made by applying a small offset potential (typically 20−50 mV) between the two electrodes. In this configuration, the device behaves as a transistor and the drain current (I_d) flowing between the electrodes is easily measured as a function of gate voltage (V_g).[17,18] It is important to note that, because I_d is directly proportional to the polymer's conductivity, measurements of the polymer's relative conductivity as a function of electrochemical potential can be easily obtained.

In this report, we have utilized this transistor configuration to measure changes in relative conductivity in two distinctly different modes. The I_d-V_g measurements measure I_d as a function of electrochemical potential (V_g). This configuration was accomplished by using a bipotentiostat, reference, and counter electrode. To allow direct comparison between I_d and redox activity, we have restricted the I_d-V_g potential ranges to lie within the potential range of the CV measurements. We have also explored a simplified electrical setup in which the polymer is first oxidized to a fixed electrochemical potential and then removed from potential control. A small potential (50 mV) is applied between the electrodes, and an in-line ammeter is used to measure changes in the current flowing through the system. It is important to note here the simplicity of this chemoresistive device with regard to the I_d-V_g experiments. Because the polymer is removed from electrochemical control, a bipotentiostat, reference, and counter electrode are not required. Although resistance measurements can also be performed under potential control, we chose to demonstrate the simplified configuration to emphasize the minimal electronics

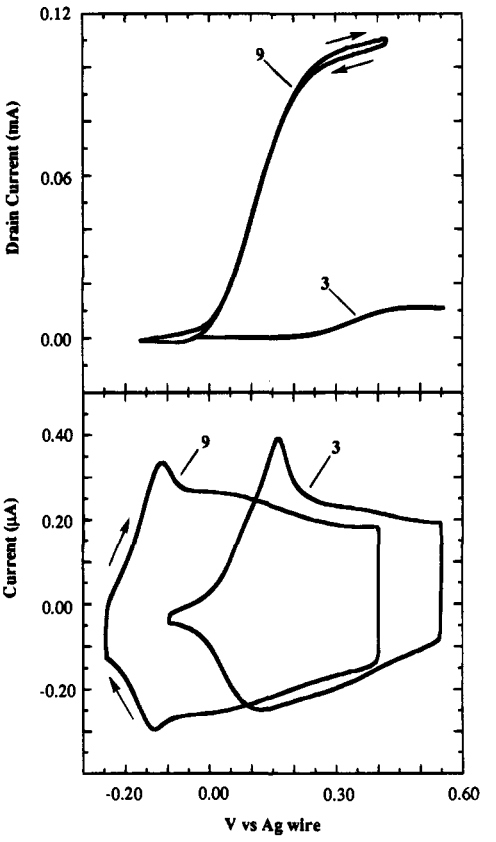

Figure 3. CV and corresponding drain current (I_d-V_g) for polymers **3** and **9**. Electrochemical measurements were made in 0.1 M $LiClO_4$/MeCN:H_2O (1:1) at a sweep rate of 50 mV/s for the CV and 25 mV/s for the I_d-V_g. The offset potential between the electrodes for the I_d-V_g was 20 mV.

required to extract a chemoresistive response. In all cases the resistance is measured in real time. Because the pseudopolyrotaxane complexes of **3** and **9** are soluble in acetonitrile, we performed our electrochemical measurements in a 1:1 mixture of water:acetonitrile, 0.1 M $LiClO_4$ with a Ag wire as reference potential. Paraquat solutions of various millimolar concentrations were made from the same electrolyte medium.

Our initial electrochemical studies focused on the inherent properties of polymers **3**, **9**, and **10**. The I_d-V_g characteristics and corresponding CVs for polymers **3** and **9** are shown in Figure 3. An important feature of Figure 3 is the significant difference observed in the magnitude of the polymer's I_ds. This difference reflects a large variation of conductivity between polymers, and saturation doping with I_2 gave absolute conductivities of 4×10^{-4}, 8×10^{-3}, and 0.9 S/cm for **3**, **9**, and **10**, respectively. Note, however, that saturation doping with I_2 does not imply that the polymers are oxidized to the potentials corresponding to their conductivity maxima as observed in the I_d-V_g characteristic of Figure 3. Polymers **9** and **10**, which are copolymerized with **7**, demonstrate a significant increase in conductivity relative to the alkyl-substituted polymer **3**. This is most likely due to the combination of steric and electronic factors previously discussed and the fact that the cyclophane receptors reduce interchain contacts. This is consistent with **10** demonstrating the highest conductivity of the series. It is noteworthy that the "turn-on" potential of conductivity for both **9** and **10** occurs at approximately −0.1 V, while **3** does not show a significant increase in conductivity until ca. +0.2 V.

Preliminary chemoresistive studies focused on the change in CV and I_d-V_g observed on addition of 50 mM paraquat, and the results for **3** and **9** are shown in Figure 4. Although our previous investigations on the interactions between **3** and

(17) Kittlesen, G. P.; White, H. S.; Wrighton, M. S. *J. Am. Chem. Soc.* **1984**, *106*, 7389.
(18) Ofer, D.; Crooks, R. M.; Wrighton, M. S. *J. Am. Chem. Soc.* **1990**, *112*, 7869.

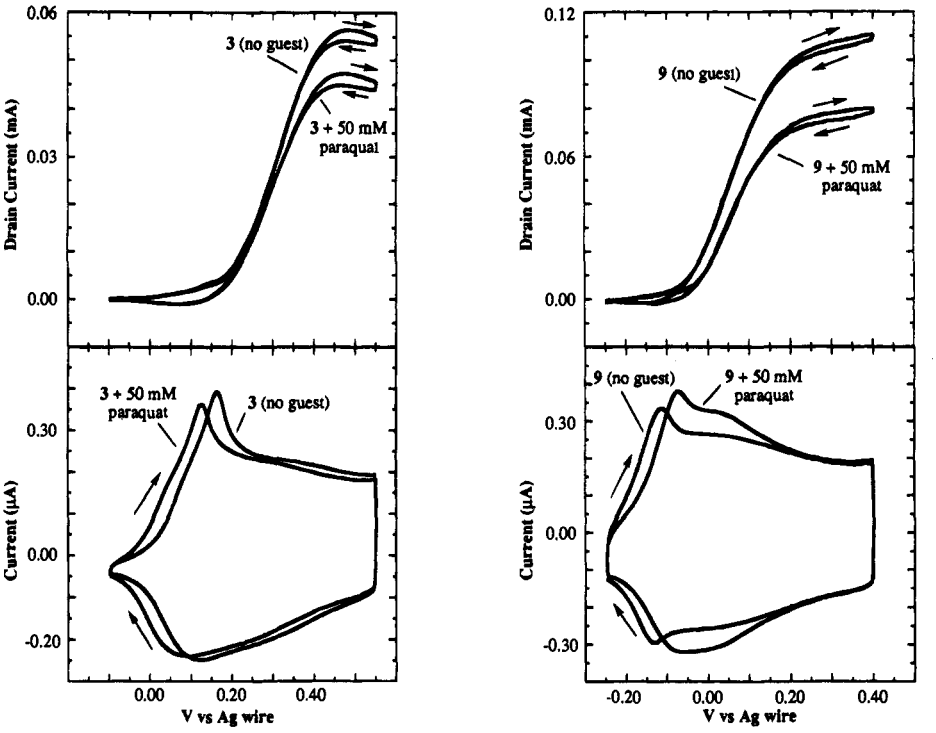

Figure 4. CV and corresponding drain current (I_d-V_g) for polymers **3** and **9** in the absence and presence of 50 mM paraquat. Electrochemical measurements were made in 0.1 M $LiClO_4$/MeCN:H_2O (1:1) at a sweep rate of 50 mV/s, for the CV and 25 mV/s for the I_d-V_g. The offset potential between the electrodes for the I_d-V_g was 20 mV.

paraquat showed no change in the redox potential,[9] we find that thinner films (ca. 1 μL of 1 mM polymer in $CHCl_3$ deposited over ca. 10 mm^2) showed a small, unexpected *negative* shift in the potential at which **3** is oxidized. This result was particularly surprising since previous studies of **3** exposed to 45 mM **4** showed a 100 mV positive shift in the potential at which **3** is oxidized. Despite this result, a 16% decrease in peak conductivity as measured by I_d-V_g experiments was observed with the addition of 50 mM paraquat.

During the course of our studies, it was observed that the relative conductivity of **3** increased after the neutral films were exposed to paraquat and then rinsed copiously with fresh electrolyte solution to remove the paraquat. Specifically, neutral films of **3** that were soaked for 12 h in a 50 mM solution of paraquat and then rinsed demonstrated a greater than 2-fold increase in relative conductivity. This effect was less noticeable in polymers **9** and **10**, but for consistency, all electrochemical measurements were performed on films that had been exposed to paraquat for a period of time such that the conductivity had reached a plateau. The origin of this effect is likely some initial degree of conformational disorder which twists the polymer's backbone away from planarity. Exposure to paraquat and subsequent pseudorotaxane formation forces disordered receptors into the desired planar transoid conformation, thereby planarizing the backbone and increasing conductivity. This effect also explains the unexpected negative voltammetric response for **3** with 50 mM paraquat. Assuming rapid exchange between occupied and unoccupied receptors, local areas of paraquat-induced increased planarity are oxidized at potentials lower than regions either conformationally unaffected by or occupied by paraquat. Although the oxidation process generates localized regions of carrier species, a decrease in conductivity is observed due to restriction of their mobility emanating from electrostatic repulsions with paraquat-occupied sites. It is important to emphasize that, while the overall advantageous increase in effective conjugation length outweighs electrostatic factors with regard to the voltammetric response, the electrostatic perturbations to carrier transport are readily detected via the chemoresistive response.

Polymer **9** demonstrated the greatest chemoresistive response (Figure 4) within the polymer series with relative conductivity decreasing by 26% on exposure to 50 mM paraquat. Unlike **3**, the decrease in relative conductivity is commensurate with a *positive* shift (40 mV) in the potential at which **9** is oxidized. These results support our assertion that "electronic tuning" the redox potential of polymer **9** to more closely match that of paraquat would manifest a larger chemoresistive response. This implies that the K_a of **9** is greater than that of **3**. This is reasonable on the grounds of both the steric hindrance arising from the decyl side chain of **3** and the electronic differences previously addressed. As such, the positive shift in the potential at which **9** is oxidized implies a greater population of paraquat-occupied receptor sites than that which is observed for **3**. This same argument is also consistent with the larger chemoresistive response exhibited by **9**.

The model polymer (**10**), which is unable to form a pseudorotaxane complex, showed no chemoresistive or voltammetric response. The combined electrochemical properties of **3**, **9**, and **10** demonstrate two important features. First, they illustrate that the chemoresistive response is a direct result of pseudorotaxane formation. Second, due to the amplification of minor defects by carrier transport properties, the chemoresistive response does not require a direct correlation to specific changes in the potential at which a polymer is oxidized or reduced.

To fully exploit the reversibility of these systems we investigated real-time devices by continuous monitoring of the conductivity of a sensory device in a flow cell as aliquots of paraquat were injected into a mobile phase. The sensory devices consist of the same microelectrode arrays used to measure I_d-V_g, differing only in the fact that they are interconnected with a polymer which has been electrochemically oxidized to its conducting state. Changes in conductivity were monitored by observing the current flowing through the system when configured in the simplified setup discussed previously. Due to

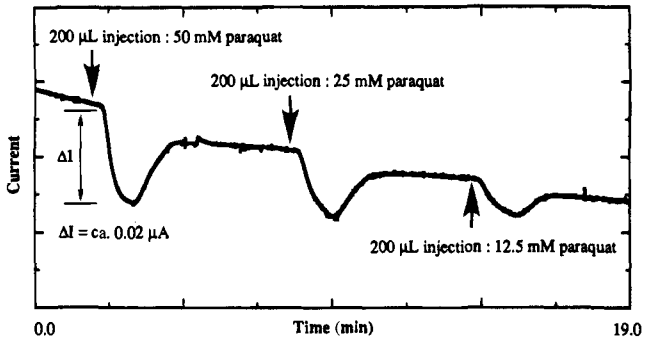

Figure 5. Chemoresistive response of a flow cell device fabricated from **9** electrochemically oxidized to −0.1 V (vs Ag wire). The plot shows the current flowing with a 50 mV offset potential between the electrodes vs time as 200 μL of paraquat solutions of variable concentration were injected into the mobile phase (0.1 M $LiClO_4$/ MeCN:H_2O (1:1), flow rate = 0.2 mL/min).

its greater inherent conductivity and chemoresistive response, devices were derivatized with polymer **9**.

Several attempts at monitoring paraquat-induced changes in resistance were made using films of **9** electrochemically oxidized to potentials greater than −0.1 V; however, at higher oxidation states, no significant chemoresistive response was observed. In order to make functional devices, films were oxidized to −0.1 V. Injection of 200 μL paraquat solutions into the mobile phase (0.20 mL/min) produced only minor changes in the resistivity of **9** (Figure 5). In no case did this chemoresistive response equal the magnitude of decrease in relative conductivity observed in the I_d-V_g characteristics. However, there clearly exists a qualitative relationship between paraquat concentration and the observed chemoresistive response. These results foreshadow the potential of these materials as real-time sensory devices, and as such, we did not concern ourselves with further optimization of the flow cell or device at this time. The sloping baseline observed in Figure 5 indicates a slight loss of electrochemical activity over time. We observed a much faster degradation of devices during these measurements than in the other configurations investigated, indicating that there may be some loss of polymer from the electrode surface resulting from solvent turbulence within the flow cell. With regard to the discrepancies observed between the magnitude of responses, we realized that these measurements differed from the I_d-V_g measurements only in the fact that the polymer was not allowed to cycle back to its neutral state. As such, we proceeded to explore the interaction between paraquat and the polymer as a function of oxidation state.

The major driving force for the self-assembly of the pseudorotaxane complex of **1** and paraquat is the charge transfer interaction between the electron-rich receptor and the electron-deficient guest. However, oxidative doping of the polymer to its conducting state results in partial positive charge residing on the thiophenes which are incorporated into the receptor site. This situation presents a paradox since oxidation is required to bring the polymer to its conducting state, yet an oxidized receptor site should inhibit pseudorotaxane formation. In an attempt to better understand this relationship, we monitored the paraquat-induced change in I_d-V_g as a function of the oxidation state of **9**.

In this investigation, the I_d-V_g was measured in real time as the concentration of paraquat increased from 0 to 50 mM. This was accomplished by continuous addition of paraquat with a syringe pump while cycling the device. Figure 6 shows the real-time I_d-V_g characteristics of polymer **9** as it is cycled repeatedly over different potential ranges. Note that, as was shown in Figure 3, the conductivity does not noticeably increase until after the polymer is significantly oxidized. For cycling between −0.25 and +0.4 V, the decrease in $I_{d\,(max)}$ is 26%. Changing the lower limit of the potential range to −0.1 V, a potential at which the peak oxidation of **9** is observed, resulted in a 14% overall decrease in $I_{d\,(max)}$. Finally, investigations which increased the lower limit of the potential range to 0 V, a potential at which the polymer (and thus the receptor sites) is significantly oxidized, demonstrated only a 5% decrease in $I_{d\,(max)}$. As was predicted, the decreased ability of paraquat to bind to the oxidized form of **9** results in a much smaller chemoresistive effect.

These results imply that oxidation of the polymers to their conducting state creates less favorable receptor sites. As a result, the population of occupied receptor sites decreases at high oxidation states of the polymer. Thus, the range of chemoresistive response observed in the I_d-V_g characteristics where the polymer is allowed to return to its neutral state is not obtainable in films maintained at their oxidized state. These interpretations also suggest that, while the binding of paraquat to the polymer is reversible, the polymer and paraquat are not in equilibrium during the I_d-V_g experiments. However, it is imperative to note that this limitation is solely a reflection of the binding affinity between receptor and guest and not an inherent limitation of chemoresistive materials. It is entirely feasible to increase the sensitivity of such materials by utilizing host−guest couples in which a positively charged receptor is required for the binding of an analyte (i.e., chemoresistive materials for the detection of electron-rich aromatics such as dopa, dopamine, etc.).[11] Regardless, the utility of chemoresistivity as a sensory probe is clearly demonstrated by the consistent decrease in conductivity observed on exposure to analyte.

Summary

We have synthesized polythiophenes containing macrocyclic receptors which are capable of reversibly forming self-assembling pseudopolyrotaxane complexes with paraquat. Polymers containing **7** as a repeat unit are oxidized at lower potentials and exhibit higher conductivities than polymers containing alkyl side chains. The electrostatic interactions occurring from sites of "pseudorotaxification" produce changes in both the polymers' conductivities and the potentials at which they are oxidized. We have found no direct correlation between analyte-induced voltammetric response and chemoresistive behavior in CPs. The sensitivity difference between these two sensory probes is addressed in the paper immediately following this one; however, herein it is evident that chemoresistivity demonstrates an increased sensitivity to electrostatic perturbations with respect to voltammetric measurements. We have successfully utilized these chemoresistive materials in the development of real-time sensory devices. The generality of our design allows for the implementation of known molecular recognition principles to produce CPs responsive to a variety of chemical entities. This generality is further exemplified in the paper immediately following this one by the successful modification of this design to produce ionoresistive calix[4]-arene-substituted polythiophenes.

Experimental Section

General Procedures. Air- and moisture-sensitive reactions were carried out in over-dried glassware using standard Schlenk techniques under an inert atmosphere of dry argon. THF was distilled from sodium−benzophenone ketyl or used directly from Aldrich Kilo-Lab metal cylinders. Pyridine was dried over molecular sieves prior to use.

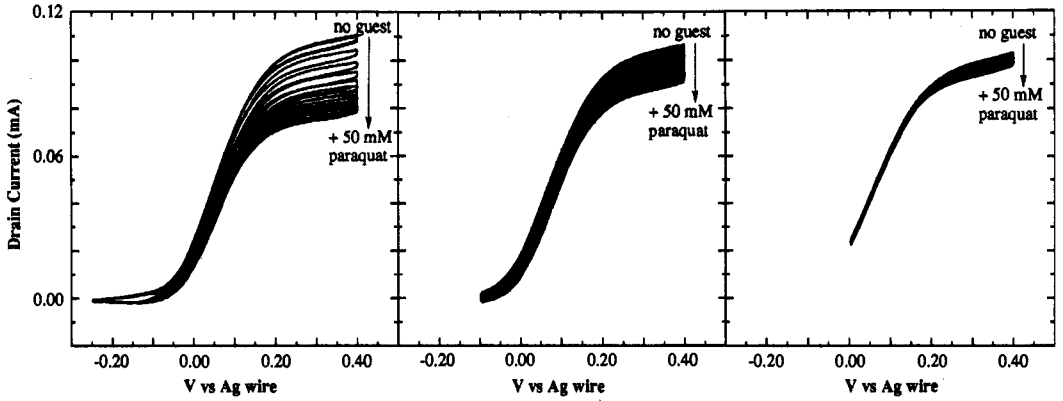

Figure 6. Drain currents (I_d–V_g) for **9** as the concentration of paraquat is increased from 0 to 50 mM for cycling over three different voltage ranges. Electrochemical measurements were made in 0.1 M $LiClO_4$/MeCN:H_2O (1:1) at a sweep rate of 25 mV/s, and the offset potential between the electrodes was 20 mV.

Reagents were used as received from Aldrich unless otherwise noted. Paraquat bis(hexafluorophosphate) was prepared from its dichloride salt (Aldrich) by counterion exchange with aqueous NH_4PF_6. NMR spectra were recorded with a Bruker AC-100 (100 MHz), AC-250 (250 MHz), or AMX-500 (500 MHz) spectrometer. GPC was performed on a Rainin HPXL solvent delivery system with a RI-1 refractive index detector and three Waters Ultrastyragel columns (10^4, 10^3, and 500 Å). Molecular weights are reported relative to polystyrene standards. UV–vis absorption spectroscopy was performed on an Olis spectrophotometer with a Cary-14 spectrophotometer conversion upgrade or a Hewlett Packard 8452A diode array spectrophotometer. Binding constants were performed in acetone and determined according to literature procedures.[11,19] Electrochemical measurements were carried out using a Pine Model RDE 3 bipotentiostat. The data were recorded on a Macintosh IIci using LabVIEW 2 (National Instruments). Microelectrode devices used in these studies were obtained from AAI-ABTECH and had an interelectrode spacing of 10 μm. All potentials were controlled relative to an isolated silver wire quasielectrode. CVs obtained by this electrochemical setup were checked for accuracy by using ferrocene samples as a reference compound in the same electrolyte medium used for the electrochemical studies. The ferrocene $E_{1/2}$ was found to be consistently at +0.14 V. Electrochemical measurements were carried out under ambient conditions in MeCN:H_2O (1:1), 0.1 M $LiClO_4$.

Preparation of 3-(11-Hydroxy-3,6,9-trioxa-1-undecoxy)thiophene (I). CuI (0.2 mol), potassium *tert*-butoxide (1.5 mol), and tetrakis(ethylene glycol) (5 mol) were added to 500 mL of pyridine and allowed to stir for 0.5 h. 3-Bromothiophene (1 mol) was added, and the mixture was heated to 100 °C for 24 h. The mixture was filtered, and the salts were washed with CH_2Cl_2. The combined organic solution was extracted with 10% HCl to remove pyridine, 10% ethylene diamine to remove copper salts, and then water. The CH_2Cl_2 layer was dried with $MgSO_4$ and then concentrated under vaccum. The crude extract was vaccum distilled (bp 180 °C at 5 mTorr) to yield the desired product in 68.5% yield as a colorless oil. ^{1}H NMR ($CDCl_3$, 100 MHz): δ 7.11 (dd, 1 H, J = 5.2, 3.0 Hz), 6.71 (dd, 1H, J = 5.2, 1.4 Hz), 6.21 (dd, 1H, J = 3.0, 1.4 Hz), 4.19–3.42 (m, 17H). ^{13}C NMR ($CDCl_3$, 25 MHz): δ 157.46, 124.41, 119.37, 97.62, 72.37, 70.59–70.21, 69.52, 61.52. HRMS: calcd 277.1109, obsd 277.1116.

Preparation of 3-(11-(Toluenesulfonyl)-3,6,9-trioxa-1-undecoxy)-thiophene (II). Toluenesulfonyl chloride (0.184 mol) was added dropwise to a 0 °C pyridine solution of **I** (0.153 mol) and allowed to stir for 6 h. The reaction mixture was then extracted (CH_2Cl_2/10% HCl), and the organic layer was concentrated under reduced pressure. The crude extract was purified by silica gel column chromatography (ethyl ether) to give the desired product in 95.3% yield as a viscous oil. ^{1}H NMR ($CDCl_3$, 100 MHz): δ 7.71 (d, 2H, J = 8 Hz), 7.24 (d, 2H, J = 8 Hz), 7.08 (dd, 1H, J = 3.0, 5.2 Hz), 6.68 (dd, 1H, J = 1.4, 5.2 Hz), 6.18 (dd, 1H, J = 1.4, 3.0 Hz), 4.11–3.50 (m, 16H), 2.35 (s, 3H). ^{13}C NMR ($CDCl_3$, 25 MHz): δ 157.46, 144.49, 133.13, 129.57, 127.64, 124.33, 119.30, 97.65, 70.49, 69.46–69.05, 68.42, 21.25. HRMS: calcd 431.1198, obsd 431.1182.

(19) Conners, K. A. *Binding Constants*; Wiley: New York, 1987.

Preparation of Compound 5. Compound II (0.146 mol) was added to a solution (150 mL of acetone/5 mL of DMF) of hydroquinone (0.073 mol) and K_2CO_3 (0.219 mol), and the mixture was allowed to reflux for 3 days. The reaction was extracted (CH_2Cl_2/H_2O), and the organic layer was dried over $MgSO_4$ and concentrated under reduced pressure. The recovered crude extract was recrystallized from ethyl ether to afford the desired product in in 95% yield. Mp: 66 °C. ^{1}H NMR ($CDCl_3$, 100 MHz): δ 7.12 (dd, 2H, J = 3.2, 5.2 Hz), 6.80 (s, 4H), 7.74 (dd, 2H, J = 1.6, 5.2 Hz) 6.24–6.19 (dd, 2H, J = 1.6, 3.2 Hz), 4.12–5.55 (m, 32H). ^{13}C NMR ($CDCl_3$, 25 MHz): δ 157.59, 153.15, 124.45, 119.46, 115.64, 97.69, 70.72–70.60, 69.77–69.62, 68.17. HRMS: calcd 626.2219, obsd 626.2210.

Preparation of Compound 1 via Route 1. BuLi (0.032 mol) was added to a 0 °C THF solution of **5** (0.016 mol), and the mixture was stirred at 0 °C for 0.5 h. THF was then added to this solution to make the total volume 250 mL. This reaction mixture was transferred at 0 °C into a refluxing THF solution (250 mL) containing $Fe(acac)_3$ (0.032 mol) and allowed to reflux for 3 h. The mixture was filtered, and the salts were washed with THF. The filtrate was concentrated under reduced pressure to yield a red oil which was purified by silica column chromatography (EtOAc) and recrystallized from EtOAc to afford **1** in 13% yield. Mp: 97–98 °C. ^{1}H NMR ($CDCl_3$, 100 MHz): δ 7.00 (d, 2H, J = 6 Hz), 6.74 (d, 2H, J = 6 Hz), 6.70 (s, 4H), 4.21–3.66 (m, 32H). ^{13}C NMR ($CDCl_3$, 25 MHz): δ 153.01, 151.70, 121.89, 116.52, 115.60, 114.74, 71.47, 70.84, 70.05–69.76, 68.15. Anal. Calcd for ($C_{30}H_{40}S_2O_{10}$): C, 57.66; H, 6.47. Found: C, 57.57; H, 6.60. HRMS: calcd 624.2063, obsd 624.2051.

THP Protection of I (III). Dihydropyran (0.175 mol) was added dropwise to a room temperature CH_2Cl_2 solution of **I** (0.0875 mol) and a catalytic amount of pyridinium *p*-toulenesulfonate. The reaction was followed by TLC, and upon completion, the mixture was extracted (CH_2Cl_2/$NaHCO_3$ (aq)). The organic layer was dried ($MgSO_4$) and concentrated under reduced pressure. The crude extract was purified by silica column chromatography (ethyl ether) to afford the desired product in 89.5% yield as a colorless oil. ^{1}H NMR ($CDCl_3$, 100 MHz): δ 7.12 (dd, 1H, J = 5.1, 3.0 Hz), 6.73 (dd, 1H, J = 5.1, 2.0 Hz), 6.21 (dd, 1H, J = 2.0, 3.0 Hz), 4.58 (m, 1H), 4.12–3.34 (m, 18H), 1.59–1.45 (m, 6H). ^{13}C NMR ($CDCl_3$, 25 MHz): δ 157.21, 124.40, 119.44, 98.81, 97.71, 70.60–70.55, 69.62, 66.56, 62.00, 30.50, 25.36, 19.35. HRMS: calcd 360.1607, obsd 360.1614.

3,3′-Bis(11-hydroxy-3,6,9-trioxa-1-undecoxy)-2,2′-bithiophene (IV). BuLi (0.055 mol) was added to a 0 °C THF solution of **III** (0.055 mol), and the mixture was stirred at 0 °C for 0.5 h. This reaction mixture was then transferred at 0 °C into a refluxing THF solution containing $Fe(acac)_3$ (0.055 mol) and allowed to reflux for 3 h. The mixture was filtered, and the salts were washed with THF. The filtrate was concentrated under reduced pressure to yield a red oil which was purified by silica column chromatography (EtOAc) to afford the desired product as a colorless oil in 69% yield. ^{1}H NMR ($CDCl_3$, 100 MHz): δ 7.15 (d, 2H, J = 5.5 Hz) 6.80 (d, 2H, J = 5.5 Hz), 4.58 (m, 2H), 4.25–3.41 (m, 36H), 1.82–1.45 (m, 12H). ^{13}C NMR ($CDCl_3$, 25 MHz): δ 151.70, 121.77, 116.54, 114.72, 98.73, 71.25, 70.72–70.47,

69.85, 69.54, 66.49, 61.89, 30.40, 25.27, 19.23. HRMS: calcd (m + Na) 741.2955, obsd 741.2970. The compound was then deprotected in MeOH using catalytic pyridinium *p*-toluenesulfonate. The reaction was followed by TLC and upon completion, the mixture was extracted (CH_2Cl_2/H_2O) and dried over $MgSO_4$ and the CH_2Cl_2 solution was concentrated under reduced pressure to afford a quantitative deprotection to give the desired product as a viscous oil. ^1H NMR ($CDCl_3$, 100 MHz): δ 7.15 (d, 2H, J = 6.0 Hz), 7.05 (d, 2H, J = 6.0 Hz), 4.26–3.43 (m, 32H). ^{13}C NMR ($CDCl_3$, 25 MHz): δ 151.67, 121.78, 116.53, 114.61, 72.35, 71.22, 70.68, 70.44, 70.18, 69.84, 69.51, 61.47. HRMS: calcd 551.1984, obsd 551.1974.

Preparation of Compound 6. Toluenesulfonyl chloride (0.015 mol) was added dropwise to a 0 °C pyridine solution (10 mL) of **IV** (6.95 mmol) and allowed to stir for 6 h. The reaction mixture was then extracted (CH_2Cl_2/10% HCl), and the organic layer was concentrated under reduced pressure. The crude extract was purified by silica column chromatography (EtOAc) to give the desired product in 77% yield as a viscous oil. ^1H NMR ($CDCl_3$, 100 MHz): δ 7.83 (d, 4H, J = 8.1 Hz), 7.35 (d, 4H, J = 8.1), 7.12 (d, 2H, J = 5.6 Hz), 6.89 (d, 2H, J = 5.6 Hz), 4.33–3.62 (m, 32H), 2.46 (s, 6H). ^{13}C NMR ($CDCl_3$, 25 MHz): δ 151.86, 144.62, 133.40, 129.72, 127.88, 121.92, 116.67, 114.81, 71.41, 70.873–70.55, 70.02, 69.16, 68.68, 21.46. HRMS: calcd (m + Na): 881.1980, obsd 881.1972.

Preparation of Compound 1 via Route 2. A solution of **4** (3.5 mmol) dissolved in 100 mL of DMF was added dropwise to a DMF solution (400 mL) of hydroquinine (3.5 mmol) and Cs_2CO_3 (3.7 mmol). The reaction was allowed to stir at 50 °C for 5 days. The reaction was diluted with CH_2Cl_2 and extracted multiple times with water to remove the DMF. The organic layer was dried over $MgSO_4$ and concentrated under reduced pressure. Silica column chromatography (EtOAc) of the crude followed by recrystallization from EtOAc afforded **9** in 17.3% yield as colorless crystals. ^1H and ^{13}C NMR and HRMS are identical to those observed for route 1.

Preparation of 3-(2-Methoxyethoxy)thiophene (V). 3-Bromothiophene was added to a lutidine solution containing 2-methoxyethanol (1.5 mol), potassium *tert*-butoxide (1 mol), and CuI (0.1 mol). The mixture was stirred and heated to 100 °C for 24 h (*CAUTION:* This reaction has occasionally produced a sudden and violent exotherm.) The reaction was then cooled and filtered. The salts were rinsed with CH_2Cl_2, and the combined organic layers were extracted with 10% HCl (aq) to remove excess lutidine. The organic layer was dried over $MgSO_4$ and concentrated under reduced pressure. The crude mixture was vacuum distilled under reduced pressure (bp 55 °C at 15 mTorr) from $CaCO_3$ to afford 3-(2-methoxyethoxy)thiophene in 78.4% yield as a colorless oil. ^1H NMR ($CDCl_3$, 100 MHz): δ 7.14 (dd, 1H, J = 3.0, 5.2 Hz), 6.77 (dd, 1H, J = 1.4, 5.2 Hz), 6.22 (dd, 1H, J = 1.4, 3.0), 4.05 (m, 2H), 3.72 (m, 2H), 3.42 (s, 3H). ^{13}C NMR ($CDCl_3$, 25 MHz): δ 157.63, 124.47, 119.47, 97.74, 70.92, 69.48, 58.92. HRMS: calcd 158.0402, obsd 158.0405.

Preparation of Compound 7. BuLi (0.32 mmol) was added to a −10 °C THF solution of **V** (3.2 mmol) containing TMEDA (3.2 mmol), and the mixture was allowed to stir for 0.5 h. This solution was transferred to a refluxing THF solution containing $Fe(acac)_3$ and allowed to stir at reflux for 6 h. The crude mixture was concentrated, redissolved in ether, and filtered through a short pad of silica. The silica was rinsed multiple times with ether. The ether rinses were combined and concentrated to produce a red oil. Crystallization from MeOH/EtOAc afforded nearly colorless crystals of 3,3′-bis(2-methoxyethoxy)-2,2′-bithiophene in 70% yield. Mp: 76 °C. ^1H NMR ($CDCl_3$, 100 MHz): δ 7.07 (d, 2H, J = 5.5 Hz), 6.83 (d, 2H, J = 5.5 Hz), 4.18 (br, 4H), 3.78 (br, 4H), 3.58 (s, 6H). ^{13}C NMR ($CDCl_3$, 25 MHz): δ 151.91, 122.00, 116.74, 115.02, 71.34, 59.09. HRMS: calcd 314.0647, obsd 314.0659.

Preparation of Compound 8. In the absence of light, compound **7** (1.6 mmol) was dissolved in CH_2Cl_2 and $Hg(OAc)_2$ (3.2 mmol) was added portionwise. The mixture was allowed to stir for 0.5 h. NIS (3.2 mmol) was then added portionwise, and the resulting mixture was allowed to stir for 0.5 h. The resulting product (both in crude and pure forms) is unstable for long periods of time if exposed to high temperatures or ambient light. As such, the reaction mixture was rapidly filtered through a short pad of silica, and the solvent was removed under reduced pressure. The resulting crude mixture was recrystallized from EtOAc to yield white crystals (60%) which rapidly developed a slight green hue. The compound was stored in the refrigerator until further use. Mp: 116 °C (dec). ^1H NMR ($CDCl_3$, 100 MHz): δ 6.95 (s, 2H), 4.17 (m, 4H), 3.74 (m, 4H), 3.44 (s, 6H). ^{13}C NMR ($CDCl_3$, 25 MHz): δ 59.21, 71.11, 71.34, 71.56, 120.29, 125.84, 151.52. Anal. Calcd for ($C_{14}H_{16}S_2O_4I_2$): C, 29.70; H, 2.85. Found: C, 29.84; H, 2.89. HRMS: calcd 566.8668, obsd 566.8653.

Preparation of Polymers 3 and 10. A typical procedure is as follows: 1 equiv of bithiophene monomer (**1** for **3** and **7** for **10**) and 10 equiv of dry LiCl were dissolved in a Schlenk tube containing THF to produce a 60 mM solution, and the Schlenk tube was then placed in a sonic bath at 0 °C. BuLi (2 equiv) was added dropwise via syringe. The mixture was kept in the sonic bath for 0.5 h while the temperature was allowed to rise from 0 °C to about 20 °C. To this mixture was added 2.2 equiv of dry $ZnCl_2$ dissolved in a minimal amount of THF. The Schlenk was then removed from the sonicator bath and stirred magnetically. Using the minimum amount of THF required to facilitate transfer, a solution containing 1 equiv of 2,5-dibromo-3-decylthiophene and approximately 3 mol % $Pd(PPh_3)_4$ was added into the flask containing the diorganozinc derivative. The solution was then heated to reflux. Several times during the course of the reaction, the volume of THF was reduced by purging dry argon through the system until a final concentration of approximately 80 mM in **1** or **7** (depending upon the polymer) was attained. The concentrated solution was allowed to reflux overnight. The polymer was precipitated in MeOH, filtered, rinsed with additional MeOH, and dried overnight under reduced pressure. Both polymers were isolated in >98% yield. **3.** ^1H NMR ($CDCl_3$, 100 MHz): δ 6.94 (br), 4.29 (br), 3.84 (br), 3.50 (br), 1.25 (br), 0.86 (br). ^{13}C NMR ($CDCl_3$, 125 MHz) including low-intensity peaks corresponding to end groups: δ 14.00, 22.55, 29.22, 29.54, 30.49, 31.05, 31.78, 67.19, 67.94, 69.63, 69.91, 70.71, 70.85, 70.92, 71.22, 71.46, 71.55, 107.15, 111.89, 112.58, 114.00, 114.43, 115.40, 122.38, 123.39, 125.72, 126.46, 127.80, 129.92, 131.84, 132.02, 132.53, 133.27, 134.47, 135.15, 140.02, 151.56, 151.76, 152.86. Anal. Calcd for $(C_{44}H_{60}O_{10}S_3)_n$: C, 62.52; H, 7.17. Found: C, 60.49, H, 7.16. **10.** ^1H NMR ($CDCl_3$, 100 MHz): δ 7.00–6.77 (br, 3H), 6.65 (br, 4H), 4.23 (br, 4 H), 4.22–3.64 (br, 28H), 1.24 (br, 18H), 0.85 (br, 3H). ^{13}C NMR ($CDCl_3$, 125 MHz) including low-intensity peaks corresponding to end groups: δ 14.04, 22.62, 29.02–29.59, 30.49, 31.85, 59.26, 71.26, 71.46, 112.08–112.75, 114.35–114.84, 116.61, 122.38–133.42, 135.24, 140.10, 143.38, 151.54–151.81. Anal. Calcd for $(C_{28}H_{38}S_3O_4)_n$: C, 62.87; H, 7.18. Found: C, 61.26; H, 7.10.

Preparation of Polymer 9. Into a Schlenk tube containing 1 equiv of **1** and 10 equiv of dry LiCl was added THF to produce a 60 mM solution. The Schlenk tube was then placed in a sonic bath at 0 °C. BuLi (2.1 equiv) was added dropwise, and the mixture was sonicated for 0.5 h while the temperature was allowed to rise from 0 °C to about 20 °C. To this mixture was added 2.2 equiv of Me_3SnCl dissolved in the minimum amount of THF required to facilitate complete transfer of reagent. The Schlenk was then removed from the sonicator bath, and the mixture was stirred magnetically. A DMF solution of 1 equiv of **8** (80 mM) and approximately 3 mol % $Pd(PPh_3)_4$ was transferred into the flask containing the diorganotin derivative of **1**, and the solution was heated to 50 °C. Dry argon was then purged through the system until all THF was removed. The concentrated solution was then heated at 120 °C overnight. **9** was precipitated in MeOH, filtered, and rinsed with additional MeOH. Further rinsing with Et_2O was repeated until no color was removed in the rinse. **9** was then dissolved in THF, precipitated in Et_2O, and dried overnight under reduced pressure to afford a 73% isolated yield. ^1H NMR ($CDCl_3$, 500 MHz): 3.46–3.49 (br), 3.64–3.67 (br), 3.70–3.94 (br), 4.21–4.30 (br), 6.65 (s), 6.69 (br), 6.90–6.93 (br). ^{13}C NMR ($CDCl_3$, 125 MHz) including low-intensity peaks corresponding to end groups: δ 59.29, 67.97, 69.68–69.95, 70.76, 71.00–71.47, 111.01–113.13, 114–115, 115.57, 132.14–133.07, 151.89, 152.95. Anal. Calcd for $(C_{44}H_{54}S_4O_{14})_n$: C, 56.50; H, 5.83. Found: C, 55.88; H, 5.74.

Flow Cell Experiment. An Alltech PEEK tee, 0.012 in. through-hole HPLC fitting was modified such that it could accomidate an AAI-ABTECH 10 μm interdigitated microelectrode, fabricated with **9** electrochemically oxidized to a given potential, in such a way that solvent flowing through the fitting would come in contact with the working surface of the electrode. This cell was configured in-line with

a Rainin HPXL solvent delivery system which allowed 0.2 mL/min of 1:1 MeCN:H_2O (0.1 M $LiClO_4$) to pass through the cell. Paraquat solutions of variable concentrations were added to the mobile phase via the HPLC injector port (200 μL injection loop), and the current flowing through the device was monitored using a Pine RDE 3 bipotentiostat configured with the counter and reference channels connected.

Acknowledgment. Funding was received from the National Science Foundation MRL program (DMR-9120668) and an NYI award to T.M.S. (DMR-9258298). T.M.S. is also grateful for funds from a DuPont Young Professor Grant and an Alfred P. Sloan Fellowship. We would like to thank Mr. Douglas M. Knawby for his assistance with designing the flow cell experiment and facilitating computer-controlled data acquisition of electrochemical measurements.

Supporting Information Available: Text giving full reports of X-ray structure determination for compounds **1** and **7** and ^1H NMR spectroscopic plots for all polymers (23 pages). This material is contained in many libraries on microfiche, immediately following this article in the microfilm version of the journal, can be ordered from the ACS, and can be downloaded from the Internet; see any current masthead page for ordering information and Internet access instructions.

JA951694S